Phase behaviour of polyethylene knotted ring chains*

Wen Xiao-Hui(温晓会)[a], Zhang Lin-Xi(章林溪)[b)†],
Xia A-Gen(夏阿根)[a], and Chen Hong-Ping(陈宏平)[a)]

[a)] *Department of Physics, Zhejiang University, Hangzhou* 310027, *China*
[b)] *Department of Physics, Wenzhou University, Wenzhou* 325027, *China*

(Received 18 July 2010; revised manuscript received 3 October 2010)

The phase behaviour of polyethylene knotted ring chains is investigated by using molecular dynamics simulations. In this paper, we focus on the collapse of the polyethylene knotted ring chain, and also present the results of linear and ring chains for comparison. At high temperatures, a fully extensive knot structure is observed. The mean-square radius of gyration per bond $\langle S^2\rangle/(Nb^2)$ and the shape factor $\langle\delta^*\rangle$ depend on not only the chain length but also the knot type. With temperature decreasing, chain collapse is observed, and the collapse temperature decreases with the chain length increasing. The actual collapse transition can be determined by the specific heat capacity $C_{\rm v}$, and the knotted ring chain undergoes gas–liquid–solid-like transition directly. The phase transition of a knotted ring chain is only one-stage collapse, which is different from the polyethylene linear and ring chains. This investigation can provide some insights into the statistical properties of knotted polymer chains.

Keywords: molecular dynamics method, phase transition, polyethylene knotted ring chain

PACS: 66.30.hk, 82.35.Lr, 87.15.rp **DOI:** 10.1088/1674-1056/20/4/046601

1. Introduction

The ability to knot is the most prominent and the least understood property of long strings, such as ropes, threads, flux lines, or polymers. For example, during the random cyclization of long polymer chains, knots of different types are formed.[1] Knots and other topological constraints are of great importance in equilibrium and dynamics properties of polymer materials, such as melts, gels and networks. Therefore, there has been considerable interest from researchers in experiments and numerical simulations in the past few years.[2,3] Knotted DNA is much easier to synthesize and to analyse than other knotted polymers,[4] and it has been identified in numerous *in vitro* and *in vivo* experiments.[5] DNA knotting probability is enhanced in P4 derivatives containing genome deletions[6] and tailless mutants. Most DNA molecules extracted from bacteriophage P4 are highly knotted because of the cyclization of the linear DNA molecule confined in the phage capsid, and DNA knots reveal a chiral organization of DNA in phage capsids. In the meantime, various types of knots are found.[7] The known set of knotted proteins is dominated by two classes: bacterial and viral rRNA methyltransferases, which make up the α/β-knot superfamily,[8] and various isozymes of carbonic anhydrase. In addition, a few other insular examples of knots in proteins have been found, one of which is ubiquitin hydraolase (UCH-3), the most complicated knot in a human protein found to date, with five projected crossings.[9] Knotted ring polymers, such as P4 DNA, can be widely observed, so the investigation of knotted polymers becomes more important.[1,4]

The coil-to-globule transition may vividly illustrate many fundamental properties of polymer systems and it has been extensively studied in the past few years.[10] Examples include the folding of proteins, the packing of DNA molecules, and the collapse of a polymer gel network as well as the complexation between two polymer chains.[11] Progress in experimental techniques has made the observation of coil-to-globule transition possible. The coil-to-globule transitions of poly (*N*-isopropylacrylamide) (PNIPAM) chains both in H_2O and in D_2O have been studied in experiments.[12] In particular, Kirwan *et al.*[13] presented the real images of coil-to-globule transitions of adsorbed poly (vinlylamine) (PVA) at different solution pHs. The complex phase behaviour of an iso-

*Project supported by the National Natural Science Foundation of China (Grant Nos. 20574052, 20774066, 20974081, and 20934004), the Program for New Century Excellent Talents in University of the Ministry of Education of China (Grant No. NCET-05-0538), and the Ph.D. Program Foundation of the Ministry of Education of China (Grant No. 20090101110002).

†Corresponding author. E-mail: Lxzhang@zju.edu.cn

© 2011 Chinese Physical Society and IOP Publishing Ltd

lated square-well chain has also been well established by Zhou *et al.*[14] The coil-globule phase behaviour transition may vividly illustrate many fundamental properties of polymer systems, therefore the study of phase behaviour transition is of considerable importance. Recently, we found that the chain topology can greatly affect the phase transition;[15,16] for example, the phase transition of polyethylene ring chains differs from polyethylene linear chains as well as the square-well and Lennard–Jones (L–J) ring chains.[15] In the present paper, we study the phase transition of polyethylene knotted ring chains, and our aim is to investigate the effects of the topological structure of ring chains on the phase transitions.

2. Model and simulation details

The united-atom (UA) force field for the polyethylene knotted ring chain is used in the present simulation: it regards each CH_2 group as a monomer. The UA force field was developed by Chang *et al.*,[17] and the advantage of this model with a significantly reduced number of degrees of freedom is that long chains or large systems can be explored within the computational limit. Recently, the UA model of polyethylene was optimized constantly and used both in MC[18] and MD simulations.[19] It has also been parameterized by first principles calculation and experimental data.[17] In fact, the UA force field model has been used successfully to deal with the elastic behaviour of ring polymer chains[20] and a single polyethylene chain confined between two adsorption walls in our previous study.[21]

In the present paper, we perform MD simulations to simulate the equilibrium properties of polyethylene knotted ring chains. The MD method has been widely used because its comparisons with theories and experiments are straightforward.[19,22−27] In the MD simulations, the motion of monomers is described by the coordinate of each monomer as a function of time. To simulate a constant temperature ensemble, the monomers are coupled to a heat bath. The collision between monomers and solvent molecules is considered and the effect is described by the Langevin equation.[22,26]

In the present simulation, the polymer system is placed in a cubic box with periodic boundary condition, the size of the box is 50σ (σ = 4.5 Å, 1 Å=0.1 nm), which represents the distance with minimum interaction energy.[15] All of the monomers are subjected to a friction force proportional to the monomer velocity. The equation of motion of the monomer is integrated by the velocity-Verlet algorithm with a time step δt,[20−25] which is set as 0.002τ. The friction constant is set to be $\Gamma = 0.5\tau^{-1}$, where $\tau = \sigma\sqrt{m/(k_{\rm B}T)}$ is the time unit.[26] In addition to MD simulations, thermal annealing is used to avoid local minima that are shown in the energy landscape of protein folding.[27] To begin with, a polyethylene knotted ring chain is generated randomly in three-dimensional (3D) space. At each temperature value during annealing, the chain relaxes sufficiently to reach thermodynamic equilibrium before equilibrium statistics are collected. In our simulation, one uses 50 temperature data, 2000 equilibrium configurations are used to calculate the thermodynamic parameters as well as 10 trajectories to obtain the final average values. Another 10 trajectories of 100-bond 3_1 knotted ring chain at T = 500 K are calculated for comparison, and the same results are obtained. Therefore, the initial structure of the knotted ring chain cannot affect the conclusions. At each temperature value, q MD steps (MDSs) are used for the chain to reach thermodynamic equilibrium, then we use another q MDSs to collect statistic properties. The relaxation time and the statistic time will be gradually increased with decreasing temperature, because the chain relaxes slowly at low temperatures. Thus, we set $q = 6q_0$ for the first 12 temperature regions; $q = 10q_0$ for the second 13 temperature regions; and $q = 16q_0$ for the third 16 temperature regions; and $q = 22q_0$ for the last 9 temperature regions. We set $q_0 = 10^6$ MDSs for the 140-bond polyethylene knotted ring chain. In order to investigate whether the chain has reached thermodynamic equilibrium, we calculate the internal

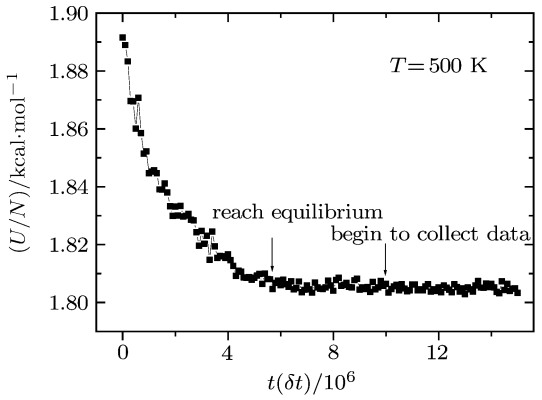


Fig. 1. Internal energy per bond U/N as a function of time for the 140-bond 3_1 knotted ring chains in the process of anealing. Here the unit of time is $\delta t(= 0.002\sigma\sqrt{m/k_{\rm B}T} = 1.65$ fs), and $t = 0$ indicates the beginning of anealing.

energy per bond U/N at different time moments. The results are given in Fig. 1. Here, the temperature is $T = 500$ K, $t = 0$ means the beginning of the annealing, and this run is chosen randomly. The internal energy per bond U/N is 1.892 (kcal/mol) at $t = 0$, and it decreases to 1.808 (kcal/mol) at $t = 5.6 \times 10^6$, when the chain has reached thermodynamic equilibrium. We begin to collect the data at $t = 10^7$ (i.e., $q = 10q_0$), therefore our results are credible.

3. Results and discussion

3.1. Chain dimensions of knotted ring chains

The average size of the polyethylene knotted ring chains can be measured by the mean-square radius of gyration per bond $\langle S^2\rangle/(Nb^2)$, in which $b = 0.153$ nm is the equilibrium bond length. For the 3_1 knotted ring chains, the ratios of $\langle S^2\rangle/(Nb^2)$ for different chain lengths of $N = 100$, 140, and 180 bonds each as a function of temperature are shown in Fig. 2. The radius of gyration is an important parameter to describe the collapse transition of the polymer systems. It has been used very well in previous studies for L–J linear and ring chains.[15,16,20,21] As seen in Fig. 2, the mean-square radii of gyration per bond of polyethylene knotted ring chains each undergo a smooth reduction with temperature decreasing, which indicates the collapse of the polymer system. At high temperatures, the values of $\langle S^2\rangle/(Nb^2)$ increase with increasing chain length, while at low temperatures the values decrease with increasing chain length. In fact, at high temperatures, the 3_1 knotted ring chains are fully extensive, so the values of $\langle S^2\rangle/(Nb^2)$ increase with increasing chain length. At low temperatures, the bond-bending and torsion potentials may strengthen the stiffness of the polymer chain, so shorter chains exhibit stronger stiffness, while longer chains exhibit stronger flexibility, therefore the values decrease with increasing chain length. In order to discuss the effects of the knot type on chain size, we take the 140-bond 4_1 knotted ring chain for comparison. At high temperatures, the values of $\langle S^2\rangle/(Nb^2)$ for the 140-bond 4_1 knotted ring chain are smaller than those of the 140-bond 3_1 knotted ring chain. However, at low temperatures, the values for both chains are identical. Obviously, at high temperatures, both are fully extensive, but due to different topological constraints, the values of $\langle S^2\rangle/(Nb^2)$ of the 4_1 knotted ring chain are smaller than those of the 3_1 knotted ring chain. Meanwhile, at low temperatures, both chains up to the same collapse state have identical values of $\langle S^2\rangle/(Nb^2)$. Here, we also take linear and ring chains for comparison, which are shown in the inset of Fig. 2. At high temperatures, the values of $\langle S^2\rangle/(Nb^2)$ of the 3_1 knotted ring chain are smaller than those of linear or ring chains. However, at low temperatures, their values are identical because they are all up to globule states.

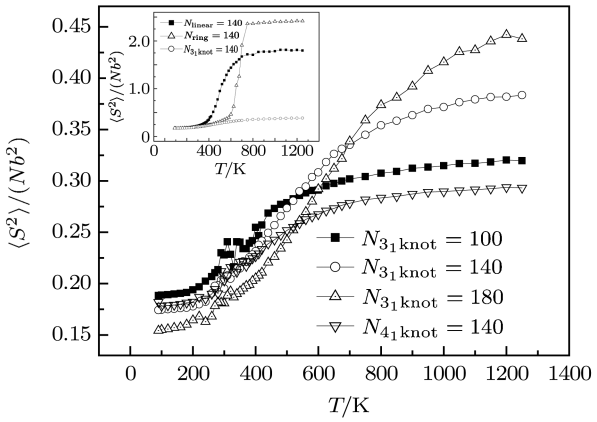


Fig. 2. Temperature dependences of the mean-square radius of gyration per bond $\langle S^2\rangle/(Nb^2)$ for knotted ring chains with $N = 100$, 140, and 180 bonds. In the inset, the results for 140-bond linear and ring chains are also presented for comparison.

In order to compare configurations of different chain sizes, the shape factor is always used, which can be obtained by combining the reduced component of S^2 to a single quantity.[15,28,29] The shape factor $\langle\delta^*\rangle$ changes between 0 (sphere) and 1 (rod).[28–32] In fact, the shape factor $\langle\delta^*\rangle$ is a parameter to depict the conformational transition. Figure 3(a) shows the temperature dependences of the shape factor of polyethylene 3_1 knotted ring chains with different chain lengths $N = 100$, 140, and 180. Meanwhile, linear, ring, and 4_1 knotted ring chains are taken for comparison. As seen in Fig. 3(a), at high temperatures, the values of $\langle\delta^*\rangle$ of the 3_1 knotted ring chains increase from 0.23 to 0.35 with the chain length increasing from $N = 100$ to 180, in which the value of the 140-bond 3_1 knotted ring chain is about 0.30, which is smaller than that of the 140-bond linear chain, but larger than that of the 140-bond ring chain, whose value of $\langle\delta^*\rangle$ is 0.25.[15] The reason for this may be that at high temperatures, the linear chain is fully extensive, the ring chain exhibits 2D oblate structure, and the knotted ring chain displays fully extensive 3D structure. Obviously, the values of $\langle\delta^*\rangle$ of the 3_1 knotted ring chain are larger than those of the 4_1 knotted ring chain for the same chain length, which is because the 4_1 knotted ring

chain has a more complex topological structure and its shape factor is relatively small. At low temperatures, the shape factors of the 3_1 knotted ring chains with different chain lengths have nearly the same values, which are close to 0.1, as well as the shape factors of 140-bond linear chain and ring chain, which also approach 0.1. At medial temperatures, such as T = 500 K$\sim$ 700 K, the values of $\langle\delta^*\rangle$ for the ring chain first increase and then decrease with decreasing temperature, which is different from those of the knotted ring chain. The temperature dependence of the shape factor for the ring chain shows that the ring chain has a two-stage phase transition, while the knotted ring chain has only a one-stage phase transition.

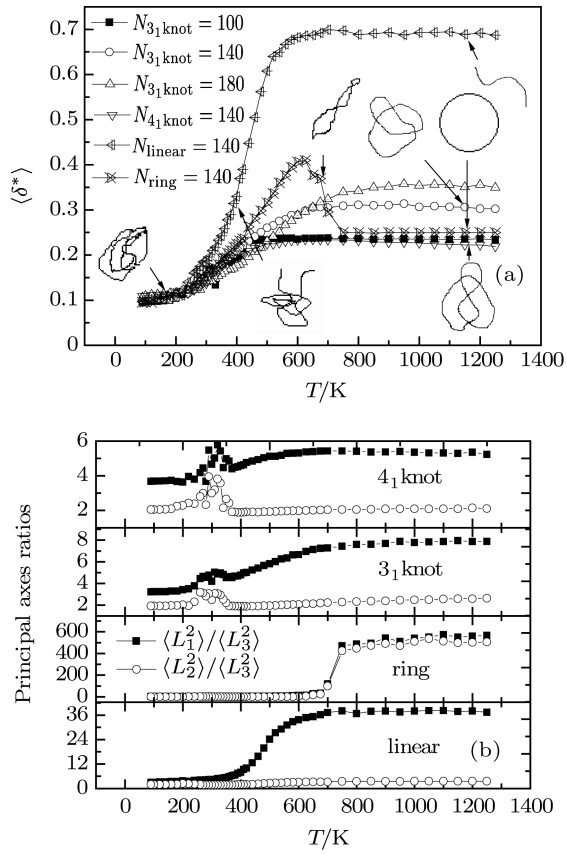


Fig. 3. Temperature dependences of the shape factor $\langle\delta^*\rangle$ (a) and the principal components (b) for knotted ring chains with different bond lengths. Here, the results for 140-bond linear and ring chains are also presented for comparison.

At low temperatures, the shape factors are all close to 0.1 for different topological structures. The three principal components L_1^2, L_2^2, and L_3^2 may well describe the configurational transitions.[28] As shown in Fig. 3(b), the ratios of the three principal components are calculated each as a function of temperature for different topological structures. For a 100-bond random walk on a simple cubic lattice, Solc and Stockmayer[28] observed a ratio of $\langle L_1^2\rangle : \langle L_2^2\rangle : \langle L_3^2\rangle$ = 11.7 : 2.7 : 1. The ratio of the polyethylene ring chain was depicted by Su and Zhang in their previous work.[15] Our result is similar to theirs. While for the 140-bond 3_1 knotted ring chain as shown in Fig. 3(b), at high temperatures, the ratio is 7.9 : 2.6 : 1, the 3_1 knotted ring chain is fully extensive in three principal directions, which may result from the chain stiffness as well as the topological constraints. With the temperature decreasing from T = 500 K to T = 360 K, there is a smooth reduction in ratio from 5.8:1.9:1 to 4.6:1.9:1. With the temperature decreasing from T = 350 K to T = 240 K, there is a sudden increase in ratio from $\langle L_1^2\rangle : \langle L_2^2\rangle : \langle L_3^2\rangle$ = 4.5 : 2.2 : 1 to $\langle L_1^2\rangle : \langle L_2^2\rangle : \langle L_3^2\rangle$ = 5.1 : 3.0 : 1, and then a sudden decrease to 3.8:2.3:1, which suggests that in the process of collapse, due to bond-bending and torsion potentials as well as topological constraints, the 3_1 knotted ring chain is extensive toward two directions, the ratio decreases with its collapse and becomes 3.2:1.9:1 at the lowest temperature T = 90 K, which approaches that of the 140-bond linear chain, thereby we say that the flexibility of the 3_1 knotted ring chain is the same as that of the linear chain. Here, we plot the ratios of the 4_1 knotted ring chain for comparison, which are shown in Fig. 3(b), with the temperature decreasing from T = 360 K to T = 260 K. There is also a sudden increase in ratio from 4.8:2.4:1 to 5.8:3.8:1, then a sudden decrease to 4.2:2.8:1. These ratios are larger than those of the 3_1 knotted ring chain, which suggests that the more complex the knot, the more easily the knot collapses to a 2D structure and the stronger its stiffness.

3.2. Collapse of knotted ring chain

More definitive information about the nature of the collapse transition can be provided by the energy properties of the knotted ring chain. The internal energy per bond $\langle U\rangle/N$ as a function of temperature for the 140-bond 3_1 knotted ring chain is shown in Fig. 4. The 140-bond linear, ring and 4_1 knotted ring chains are also shown in Fig. 4 for comparison. For the linear chain, the values of $\langle U\rangle/N$ decrease monotonically with temperature decreasing as a whole. There is a critical region between T = 200 K and T = 400 K, which is in accordance with the critical regions of $\langle S^2\rangle/(Nb^2)$ and $\langle\delta^*\rangle$ above; while for

the 140-bond ring chain, there is a large energy barrier at $T = 675$ K, which leads to a drastic conformational transition for the 140-bond ring chain, which is the first-order-like transition. However, for the 140-bond knotted ring chain, one can see only one-stage transition in Fig. 4. This phenomenon is consistent with the behaviours of $\langle S^2\rangle/(Nb^2)$ and $\langle\delta^*\rangle$ above. At a high temperature of $T = 1250$ K, the values of $\langle U\rangle/N$ for the 140-bond linear, ring, 3_1, and 4_1 knotted ring chains are 6.02, 2.84, 4.56 and 4.47, respectively. Obviously, the linear chain has the largest internal energy per bond, while the ring chain has the smallest one. The value of $\langle U\rangle/N$ of 3_1 knotted ring chain is a little larger than that of 4_1 knotted ring chain. With temperature decreasing from $T = 625$ K to $T = 260$ K, the $\langle U\rangle/N$ curve of the knotted ring chain is close to that of the ring chain, but smaller than that of the linear chain until the temperature decreasing from $T = 140$ K to $T = 90$ K, in which the curves for the four types of chains are close to each other. In particular, with the temperature decreasing from $T = 400$ K to $T = 260$ K, there are energy barriers for ring chain, 3_1 and 4_1 knotted ring chains, which are the second-order-like transition for ring chain and the one-stage transition for knotted ring chain. Due to the topological constraints of the knotted ring chain, the first-order-like transition (from oblate structure to helix structure) vanishes, directly collapsing from extensive state to globule state. We conclude that the transition of the knotted ring chain is different from that of the ring chain based on the internal energy per bond $\langle U\rangle/N$ as a function of temperature.

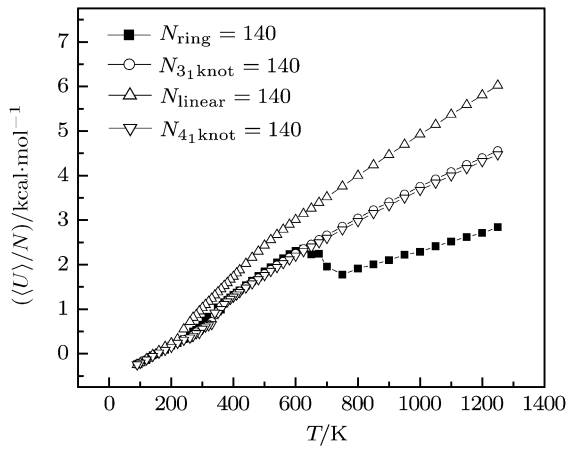


Fig. 4. Temperature dependences of the internal energy per bond $\langle U\rangle/N$ for 140-bond ring and knotted ring chains. Here, the results for the 140-bond linear chains are also presented for comparison.

It is difficult to determine the exact critical temperature based on $\langle S^2\rangle/(Nb^2)$, $\langle\delta^*\rangle$, and $\langle U\rangle/N$. In fact, Zhou *et al.*[14] have used the reduced heat capacity $C_{\rm v}$ to determine the specific transition temperatures according to Eq. (1)

$$C_{\rm v} = \frac{\langle U^2\rangle - \langle U\rangle^2}{k_{\rm B}\,T^2}, \tag{1}$$

where U is the total energy, the canonical averages $\langle U^2\rangle$ and $\langle U\rangle^2$ are evaluated using the annealing MD method. Peaks in the $C_{\rm v}$–T curve are used to identify configuration changes in the system. The heat capacities per bond $C_{\rm v}/N$ each as a function of temperature for 100-, 140-, 180-bond knotted ring chains are shown in Fig. 5(a). Their peaks are $T_{\rm C} = 370$ K, 340 K and 300 K, respectively. The critical point $T_{\rm C}$ decreases with increasing chain length. For the same topological constraints, the longer the chain length, the more flexible it is. So, it needs a lower temperature to reach the globule state for a longer knotted ring chain. From Fig. 5(a), we know that the phase transition of the knotted ring chain is a one-stage transition because there is only one peak region. To further discuss this phenomenon in more detail, we also plot the $C_{\rm v}/N$ curves of 140-bond linear, ring, and 4_1 knotted ring chains for comparison. For the linear chain, there is a high temperature shoulder at about $T = 440$ K as well as a strong peak at a low temperature ($T = 240$ K). Similar heat capacity curves were observed previously by Zhou *et al.*[14] for linear square-well chains. According to their discussion, the high temperature shoulder should represent a condensation-like collapse transition, i.e., a gas–liquid-like transition. The low temperature peak marks a liquid-solid-like ordering transition. For the 140-bond ring chain, there are two strong peaks, as seen in Fig. 5(b). The first peak is at a high temperature ($T = 675$ K) and the second peak is at a low temperature ($T = 280$ K). Similar heat capacity curves were observed previously.[15] The ring chains take a two-stage collapse transition, i.e., gas–liquid-like and liquid-solid-like transitions.[15] Because of topological constraints, with temperature decreasing, the ring chain collapses into a U-turn structure first, and then shrinks to a globule state at lower temperatures. For the 4_1 knotted ring chain, there is also a critical region in the $C_{\rm v}/N$ curve, which is similar to the scenario for the 3_1 knotted ring chain. The transition peak is at $T = 340$ K, too. Therefore, one can say that the knotted ring chain has only one-stage

phase transition, which is different from linear and ring chains.

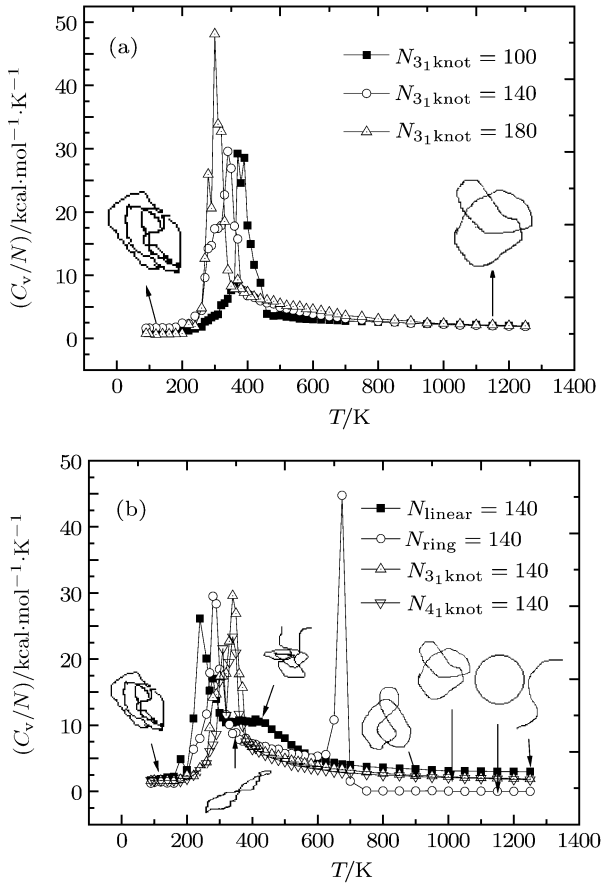


Fig. 5. (a) Temperature dependences of the heat capacity per bond C_v/N for knotted ring chains with $N = 100$, 140, and 180 bonds, and (b) results for 140-bond linear, ring, and 4_1 knotted ring chains are also presented for comparison.

The possible conformational transitions for 140-bond 3_1 and 4_1 knotted ring chains as well as 140-bond ring and linear chains are shown in Fig. 6. In Fig. 6, the 140-bond linear chain is in an extended coil state with a large end-to-end distance at high temperatures. With decreasing temperature, the linear chain collapses into a compact structure with tails, and it further collapses into a more compact torus globule at a lower temperature. For the 140-bond ring chain, it exhibits fully oblate structure at high temperatures, with decreasing temperature. It folds a few times along a nearly straight line to form abrupt U-turns near the ends like hairpins. After the liquid–solid-like transition, the 140-bond ring chain collapses into a torus-like globule, which is similar to the structure of the linear chain at the same temperature. For 3_1 and 4_1 knotted ring chains, at high temperatures, both are more extended. At low temperatures, they collapse into more compact torus globules. Obviously, there is only a one-stage transition for the knotted ring chain. We can see that the transition process of the knotted ring chain is different from those of the linear and ring chains. This conclusion is consistent with the discussions of $\langle S^2\rangle/(Nb^2)$, $\langle\delta^*\rangle$, $\langle U\rangle/N$, and C_v/N above. This 3D coordinate plot clearly exhibits the process of the phase transitions.

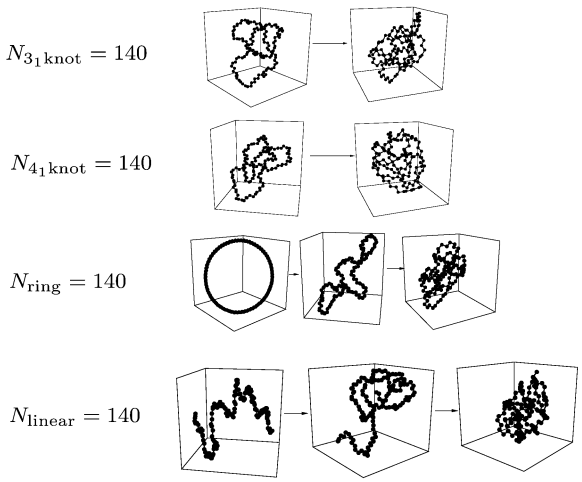


Fig. 6. The 3D coordinate plots of the 140-bond knotted ring chains during the collapse transition. The structures of 140-bond ring and linear chains are also presented for comparison.

4. Conclusions

In this paper, we have presented the collapse transitions of polyethylene knotted ring chains using MD simulation. A results comparison between linear and ring chains is made. The Langevin equation is used to mimic the collision of solvent molecules. The collapse of the linear chain is in accordance with the previous studies for square-well chains and L–J homopolymers. The linear chain undergoes a two-stage collapse transition, i.e., the gas–liquid-like and liquid–solid-like transitions. These transitions are determined by a high temperature shoulder and a low temperature peak in the heat capacity curve, respectively. The ring chain undergoes two abrupt transitions, and there are two sharp peaks in the heat capacity curve. The reason for this may be that besides the L–J and bond-stretching potentials, the bond-bending and torsion potentials are included for the polyethylene ring chain in the UA model. The bond-bending and torsion potentials should turn the ring chain into a stifflike chain, which

is different from the square-well and L–J homopolymers ring chains, and the continuous space model should be more suitable for a stifflike ring chain than the lattice model. The polyethylene knotted chain has only a one-stage transition, i.e., the knotted ring chain undergoes a gas–liquid–solid-like transition directly. At high temperatures, a fully extensive knot structure is observed. The mean-square radius of gyration $\langle S^2\rangle/(Nb^2)$ and shape factor $\langle\delta^*\rangle$ depend on not only the chain length but also the knot type. With decreasing temperature, collapse of a low temperature region is observed. The collapse temperature decreases with increasing chain length. Comparing 3_1 and 4_1 knotted ring chains, we find that the gas–liquid–solid-like transition does not depend on the knot type. This investigation can provide some insights into the conformational properties of knotted polymers.

References

[1] Rybenkov V V, Cozzarelli N R and Vologodskii A V 1993 *Proc. Natl. Acad. Sci. USA* **90** 5307

[2] Arsuaga J, Vazquez M, McGuirk P, Trigueros S, Sumners D W and Roca J 2005 *Proc. Natl. Acad. Sci. USA* **102** 9165

[3] Matthews R, Louis A A and Yeomans J M 2009 *Phys. Rev. Lett.* **102** 088101

[4] Liu L F, Depew R E and Wang J C 1976 *J. Mol. Biol.* **106** 439

[5] Wasserman S A and Cozzarelli N R 1986 *Science* **232** 951

[6] Wolfson J S, McHugh G L, Hooper D C and Swartz M N 1985 *Nucleic Acids Res.* **13** 6695

[7] Virnau P, Mirny L A and Kardar M 2006 *PLoS Comp. Biol.* **2** 1074

[8] Murzin A G, Brenner S E, Hubbard T and Chothia C 1995 *J. Mol. Biol.* **247** 536

[9] Misaghi S, Galardy P J, Meester W J N, Ovaa H, Ploegh H L and Gaudet R 2005 *J. Biol. Chem.* **280** 1512

[10] Ivanov V A, Paul W and Binder K 1998 *J. Chem. Phys.* **109** 5659

[11] Zhang G Z and Wu C 2001 *J. Am. Chem. Soc.* **123** 1376

[12] Wang X H and Wu C 1999 *Macromolecules* **32** 4299

[13] Kirwan L J, Papastavrou G, Borkovec M and Behrens S H 2004 *Nano. Lett.* **4** 149

[14] Zhou Y Q, Hall C K and Karplus M 1996 *Phys. Rev. Lett.* **77** 2822

[15] Su J Y, Zhang L X and Liang H J 2008 *J. Chem. Phys.* **129** 044905

[16] Su J Y and Zhang L X 2007 *Polymer* **48** 7419

[17] Chang J, Han J, Yang L, Jaffe R L and Yoon D Y 2001 *J. Chem. Phys.* **115** 2831

[18] Foteinopoulou K, Karayiannis N C, Mavrantzas V G and Kröger M 2006 *Macromolecules* **39** 4207

[19] Koyama A, Yamamoto T, Fukao K and Miyamoto Y 2001 *J. Chem. Phys.* **115** 560

[20] Shen Y and Zhang L X 2005 *J. Polym. Sci.* Part B: *Polym. Phys.* **43** 223

[21] Su J Y and Zhang L X 2008 *J. Polym. Sci.* Part B: *Polym. Phys.* **46** 370

[22] Lin S L, Numasawa N, Nose T and Lin J P 2007 *Macromolecules* **40** 1684

[23] Jiang S C, Zhang L X, Xia A G, Chen H P and Cheng J 2010 *Chin. Phys.* B **19** 018106

[24] Su J Y and Zhang L X 2008 *Chin. Phys.* B **17** 3115

[25] Jiang S C, Zhang L X, Xia A G and Chen H P 2010 *Acta Phys. Sin.* **59** 4337 (in Chinese)

[26] Wei Y F and Hsiao P Y 2007 *J. Chem. Phys.* **127** 064901

[27] Chen Y T, Zhang Q and Ding J D 2006 *J. Chem. Phys.* **124** 184903

[28] Solc K and Stockmayer W H 1971 *J. Chem. Phys.* **54** 2756

[29] Jagodzinski O, Eisenriegler E and Kremer K 1992 *J. Phys.* I **2** 2243

[30] Zhang L X, Sun T T, Cheng J and Ma H Z 2007 *Polymer* **48** 3013

[31] Wang Y and Zhang L X 2007 *J. Polym. Sci.* Part B: *Polym. Phys.* **45** 2322

[32] Zhang L X and Su J Y 2006 *Polymer* **47** 735